Femtosecond stimulated Raman scattering in pressurized gases in the ultraviolet and visible spectral ranges

Vitaly Krylov, Olavi Ollikainen, and Urs P. Wild

Physical Chemistry Laboratory, Swiss Federal Institute of Technology, ETH-Zentrum, CH-8092 Zurich, Switzerland

Aleksander Rebane

Department of Physics, Montana State University, Bozeman, Montana 59717

Victor G. Bespalov and Dmitry I. Staselko

S. I. Vavilov State Optical Institute, 199034 St. Petersburg, Russia

We investigate femtosecond stimulated Raman scattering (SRS) in H_2, D_2, HD, and CH_4 excited with 300-fs-duration pulses at 390-nm wavelength and with as much as 0.1 mJ of energy. We show that the SRS-generation threshold and conversion efficiency are due to the transient nature of SRS in femtosecond regime. We determine optimal conditions for efficient generation in the broad spectral range 289–797 nm and show how self-phase modulation and white-light generation limit the ultimate conversion efficiency. © 1998 Optical Society of America [S0740-3224(98)00912-6]

OCIS codes: 190.2620, 190.5650, 190.5890.

1. INTRODUCTION

In recent years there has been a rapid development of lasers that generate high-intensity ultrashort pulses. This development has prompted renewed interest in techniques of nonlinear frequency conversion of ultrashort pulses. One of the most attractive ways to convert laser light from one wavelength into a broad range of wavelengths is to use stimulated Raman scattering (SRS). Besides providing for high conversion efficiency, a special property of SRS is that one can use it to obtain coherent light simultaneously at several wavelengths. One can manipulate the exact values of these multiple Raman wavelengths and their relative intensities to a large degree by varying the active medium and by choosing from among several rotational and vibrational types of interaction.

Among known Raman-active media, the most suitable for frequency conversion of intense femtosecond pulses appear to be pressurized molecular gases such as hydrogen, deuterium, and methane.[1] These gases possess several favorable properties, including large values of rotational and vibrational Stokes frequency shifts, high degrees of optical homogeneity, and relatively low dispersion of group velocity for ultrashort pulses. In addition, these gases are photochemically stable, they are not chemically aggressive, and one can vary their optical and spectral parameters by changing the pressure.

Previously hydrogen gas was used for generation of nanosecond-duration bandwidth-limited pulses with conversion efficiencies as large as 50%.[1–3] In the femtosecond domain, the SRS experiments reported so far concern mostly generation of selected Raman components in H_2 and CH_4.[4–6] Recently[7] we performed experiments in which we investigated generation of vibrational, rotational, and rotational–vibrational Raman components in pressurized H_2 by using as the pump source 200-fs-duration 390-nm-wavelength pulses from a frequency-doubled commercial regenerative amplified Ti:sapphire laser system. With this pump source it is feasible to obtain ultrashort SRS pulses in many different Stokes and anti-Stokes spectral components. By tuning the wavelength of the frequency-doubled Ti:sapphire laser in the interval 360–425 nm one can potentially cover the whole range from 280 to 630 nm.

In this paper we investigate several gases to achieve maximum broad-wavelength coverage for SRS generation without the need to change the wavelength of the pump source. We perform, for the first time to our knowledge, a comprehensive study of femtosecond SRS in the gases H_2, D_2, CH_4, and HD. Our objective is to characterize spectral and temporal properties of various Raman components as a function of gas pressure and excitation intensity.

First we give a summary of the theoretical description of Raman gain that is relevant to a strongly transient regime. Then we discuss experimental results of measurements with femtosecond excitation pulses of SRS in several gases.

2. EVALUATION OF TRANSIENT SIMULATED RAMAN SCATTERING GAIN COEFFICIENT FOR SEVERAL GASES

Here we provide the theoretical background for understanding SRS threshold and amplification in the transient regime. Strongly transient SRS occurs when the

0740-3224/98/122910-07$15.00

duration of the pump pulse τ_p is much shorter than the vibrational and rotational dephasing time T_2 of the gas molecules, $\tau_p \ll T_2$. In this case the nonlinear polarization of the medium does not reach steady state within the duration of the excitation pulses.[8] With ultrashort-pulse excitation, phonon decay and dephasing during the pump pulse can be neglected. With the assumption of low depletion of the energy of the pump pulse, the intensity of Stokes beam at the output of the medium can be expressed as[8,9]

$$I_s \sim I_0 \exp\left\{\left[\frac{8g}{T_2}\int_0^L\int_0^{\tau_p} I_p(z,\,t)\mathrm{d}z\,\mathrm{d}t\right]^{1/2}\right\}, \tag{1}$$

where I_p is the intensity of the pump pulse, I_0 is the initial Stokes intensity, and g is the steady-state plane-wave gain coefficient. The integration of the pump intensity is performed here over the length of interaction, $z = (0, L)$, and over the duration of the excitation pulse, $t = (0, \tau_p)$. For a diffraction-limited Gaussian beam[10]

$$I_s \sim I_0 \exp\left[\left(\frac{16\pi g W_p}{T_2\lambda_p}\right)^{1/2}\right], \tag{2}$$

where the pump energy is

$$W_p = \int_{-\infty}^{\infty} P(t)\mathrm{d}t \tag{3}$$

and $P(t)$ is the instantaneous pump power.

Note that for a focused pump beam the steady-state regime SRS threshold depends on the pump power,[11] whereas the transient regime SRS threshold depends on the pump energy. If the steady-state gain g and the molecular dephasing time T_2 are both known, we can use relation (2) to evaluate the gain for the transient regime. To find the generation threshold we use the same approach as for the steady-state regime, which consists in the assumption that the required gain to reach the SRS generation threshold by amplification of vacuum field fluctuations is $\sim e^{23}$.[12] The threshold energy for transient SRS then becomes

$$W_{\mathrm{tr}} = \frac{10.5 T_2 \lambda_p}{g}. \tag{4}$$

However, using Eq. (4) requires that we know the values of parameters g and T_2 as a function of gas pressure. Unfortunately, reliable numerical values are not available for all molecules studied (H_2, HD, D_2, and CH_4) or for all pressures (1×10^6–4.5×10^6 Pa) and excitation wavelengths (390 nm) used in our experiments. To compensate for this deficiency we use a different approach in which we calculate g and T_2 from other known molecular parameters.[13–19] The results of the calculations are presented in Table 1.

As the last step, we evaluate the group-velocity mismatch (GVM) Δv between the pump wave and the Stokes wave:

$$\Delta v = \frac{1}{u_p} - \frac{1}{u_s} = \frac{1}{c}\left(n_p - n_s - \lambda_p \frac{\mathrm{d}n_p}{\mathrm{d}\lambda_p} - \lambda_p \frac{\mathrm{d}n_s}{\mathrm{d}\lambda_s}\right), \tag{5}$$

where u_p and u_s are the group velocities for the pump and the Stokes wavelengths, respectively, and $n_p - n_s$ is the corresponding difference between the linear refractive indices of the pump and the Stokes waves. For our gases, and at normal conditions ($T = 300$ K, $p = 10^5$ Pa) Cauchy's dispersion formula yields[20]:

$$n - 1 = A_1\left(1 + \frac{B_1}{\lambda^2}\right), \tag{6}$$

where A_1 and B_1 are constants. By substituting Eq. (6) into Eq. (5) and by accounting for the Lorentz–Lorenz formula ($n - 1 \propto p$), we finally obtain

$$\Delta v = \frac{pA_1B_1}{c}\left(\frac{1}{\lambda_p{}^2} - \frac{1}{\lambda_s{}^2}\right) = \frac{pA_1B_1}{c}\left(\frac{2\nu_{\mathrm{ph}}}{\lambda_p} - \nu_{\mathrm{ph}}{}^2\right), \tag{7}$$

where we have introduced the Raman frequency shift ν_{ph}. The value of coefficient A_1B_1 can be found from the literature, at least for some of our gases: H_2, 1.02×10^{-14}; D_2, 1.13×10^{-14}; and CH_4, 6.03×10^{-14}.[21] For HD, however, no literature value was found. In the region of normal dispersion the GVM depends both on the pump wavelength and on the frequency shift. In particular, it follows from Eq. (7) that the GVM between the first Stokes and the first anti-Stokes is approximately double that between the pump and the first Stokes. This circumstance is important for generation of higher Stokes and anti-Stokes components.

Table 1 summarizes the values of steady-state gain coefficient and the molecular dephasing time, which we then use to evaluate the SRS generation threshold for four gases for excitation wavelength $\lambda_p = 390$ nm and pressure $p = 3 \times 10^6$ Pa. The table also gives calculated values of GVM for purely vibrational SRS.

By analyzing the data presented in Table 1 we can draw certain conclusions about the character of transient SRS compared with that of the well-known stationary regime. First, in the stationary regime the generation

Table 1. Summary of Spectroscopic Parameters of Four Gases for SRS at Pressure $p = 3 \times 10^6$ Pa and Excitation Wavelength $\lambda_p = 390$ nm

Gas	Vibrational/ Rotational Stokes Shift $\Delta\nu$ (cm^{-1})	Steady-State Gain Coefficient g (cm/GW)	Dephasing Time T_2 (ps)	GVM (fs/cm)	Experimental SRS Threshold (μJ)	Theoretical SRS Threshold (μJ)
H_2	4155/587	4.72	203	2	27	20
HD	3631	0.13	15	–	65	50
D_2	2997/414	0.79	88	1.6	32	23
CH_4	2917	1.2	16	8.7	12	6

threshold differs from one gas to another by as much as a factor of 40, with H_2 having the lowest value. In the transient regime, however, the lowest threshold energy is in CH_4, whereas all the gases listed in Table 1 have rather similar threshold values. In particular, in the stationary regime the ratio between the threshold in H_2 and HD is ~40, whereas in the transient regime this ratio is only 2.5.

Also, both H_2 and D_2 possess narrow SRS lines and exhibit a strong dependence on pressure. In the stationary regime the SRS threshold is practically independent of the gas pressure in the range 3×10^6–5×10^6 Pa, whereas in the transient regime we can expect that the threshold will increase as the gas pressure is decreased. This circumstance can create certain difficulties in using rotational Raman components, which in the case of the stationary regime are known to be most efficiently excited at pressures of 10^5–10^6 Pa.[22]

3. EXPERIMENTAL RESULTS AND DISCUSSION

A schematic of our experimental setup is shown in Fig. 1. We used a commercial femtosecond Ti:sapphire regenerative amplifier system[23] to generate 200-fs-duration pulses at the 780-nm wavelength and a pulse energy of 0.75 mJ at a 1-kHz repetition rate. Frequency doubling was performed in a 2.5-mm-thick KDP crystal. The energy of the pulses at 390 nm was 0.3 mJ, and the pulse duration was 300 fs. The gas cell was a stainless-steel cylinder with 25-mm-diameter quartz windows of two different lengths, 30 and 100 cm. The gas pressure varied in the range 10^6–9×10^6 Pa.

We varied the pump intensity by attenuating the pulses with neutral-density filters. We also changed the focusing conditions in the Raman cell by using spherical lenses with focal lengths $f = 25, 50, 100, 200$ cm and a telescope with variable beam-compression factors of 2×, 3×, and 4×.

Although focusing conditions do not enter directly into Eq. (5), which describes the amplification process, we observed that focusing had a profound effect on the efficiency of SRS, basically because of the self-phase modulation and the white-light-continuum generation that occur at high peak intensities. In particular, we observed that for strong focusing with a short focal-length lens the white-light-continuum generation developed before the SRS threshold was reached. Without focusing, however, at our excitation intensities of ~10 GW cm^{-2} the SRS generation threshold could not be reached. Thus we used weak focusing, so the threshold for SRS was reached before generation of the white-light continuum. Empirically, we achieved the best conversion by using a 100-cm-long Raman cell and by focusing the pump beam in the center of the cell with an $f = 100$ cm lens or by using a 4× focusing telescope.

To vary the pressure in H_2, D_2, and CH_4 we used the range 10^6–7×10^6 Pa. In the case of HD the highest pressure was limited to 2.5×10^6 Pa, as recommended by the suppliers of the gas to avoid chemical decomposition of the molecules.

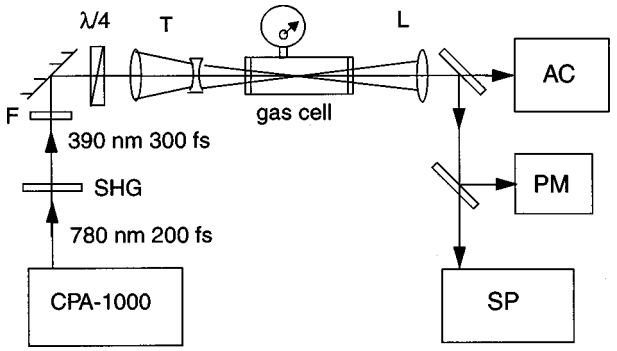

Fig. 1. Schematic of the experimental arrangement: CPA-1000, Clark MXR Model CPA 1000 1-kHz regenerative amplified femtosecond Ti:sapphire laser; SHG, β-barium borate crystal for second-harmonic generation; F, variable neutral-density attenuator; T, focusing telescope; L, collimating lens; PM, powermeter; AC, autocorrelator; SP, grating spectrometer.

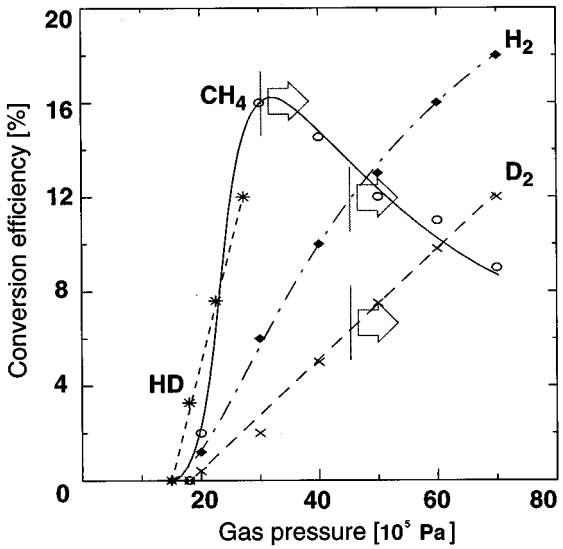

Fig. 2. Energy conversion efficiency to the first vibrational Stokes component as a function of gas pressure for four gases. The pump pulse energy at 390-nm wavelength is 0.1 mJ. Arrows indicate the threshold of white-light-continuum generation.

In the first experiment we investigated the dependence of the conversion efficiency into the first Stokes as a function of pressure. Inasmuch as both thresholds, for SRS as well as for white-light generation, increase with decreasing pressure, we are particularly interested in achieving efficient SRS without competition from the white-light-generation process. Figure 2 shows the measured dependence in four gases when the energy of the pump pulses was held constant at $W_p = 0.1$ mJ. At this pump power there is a limited range of pressure values, where the SRS generation starts before the white-light generation. In this range the maximum efficiency is 6–16%. However, the absolute maximum efficiency of 12–18% is reached at higher pressures when the white light is already present. This result is in agreement with our previous results for H_2,[7] for which the efficiency of 15% was achieved when the energy of the pump pulses was 0.4–0.6 mJ and the duration of the pump pulses was 300 fs.

From this measurement we conclude that nonlinear index of refraction n_2 of the Raman medium, which was ne-

glected in the simple description given above, gives rise to significant competing nonlinear effects. The fact that the white-light-generation threshold is similar for H_2 and D_2 at $\sim 4.5 \times 10^6$ Pa indicates that n_2 has similar magnitudes in both media. In comparison, the white-light generation in CH_4 begins at a pressure of 3×10^6 Pa.

For H_2 and D_2 the conversion efficiency increased almost linearly with the increase of pressure, whereas in CH_4 we observed a distinct maximum in the range of 3×10^6 Pa beyond which the efficiency started to decrease. A possible explanation for such different behavior can perhaps be found in the dispersion of group velocities, which in CH_4 is ~ 8.6 fs cm^{-1}. In a 100-cm-long cell, this value corresponds to a maximum time mismatch between the pump and the SRS pulse of ~ 800 fs. Even if we consider that the actual interaction length in the cell is much less than 100 cm, it appears to be sufficiently large to influence the efficiency of conversion. Another possible explanation for the bend-over in the CH_4 curve is that it is due to the lower white-light-generation threshold. It may turn out that stronger self-phase modulation in this gas impedes buildup of a SRS wave.

The result discussed above allows us to determine optimal pressure, which for given types of molecules is 4.5×10^6 Pa for H_2 and D_2, 3×10^6 Pa for CH_4, and 2.6×10^6 Pa for HD. Figure 3 shows how the efficiency varies with the energy of the pump pulses, once the optimal pressure is selected. In the case of H_2, D_2, and CH_4 the curves exhibit characteristic saturation behavior, showing more- and less-pronounced regions with fast and slow dependence, respectively, on the pump energy. Similar dependencies were observed earlier[6]; the occurrence of slow-growth regions was associated with nonlinear effects that were due to self-phase modulation of the pump pulses. The absence of a flattening out of the curve obtained in HD can be explained by a higher threshold of SRS generation, which would limit the conversion efficiency in the given pump pulse energy range.

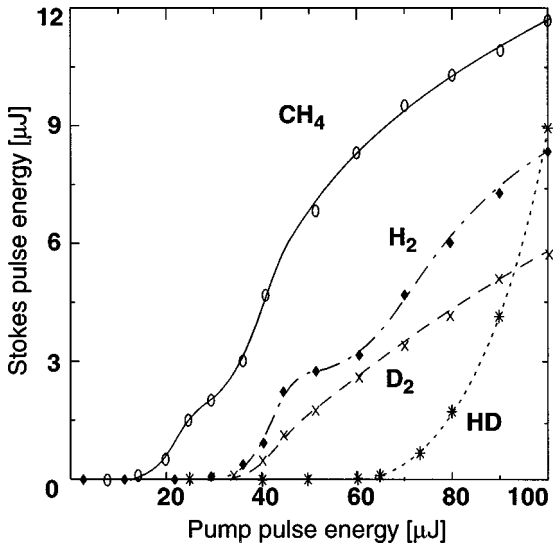

Fig. 3. Dependence of energy of the first vibrational Stokes pulse on the pump pulse energy for four gases. Gas pressure: in CH_4, 3×10^6 Pa; in H_2, 4.5×10^6 Pa; in D_2, 4.5×10^6 Pa; in HD, 2.6×10^6 Pa.

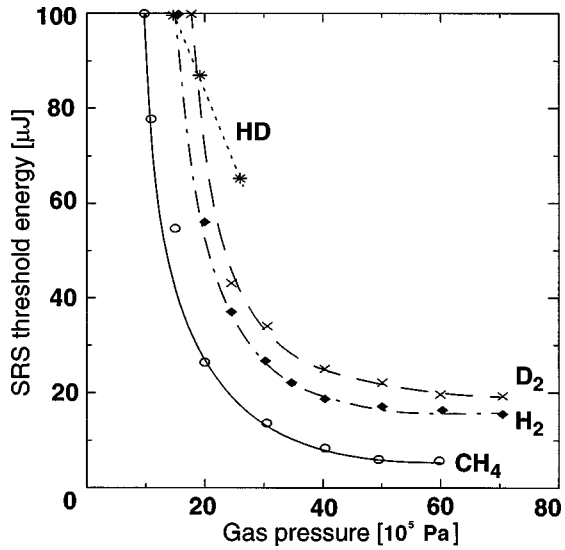

Fig. 4. Dependence of SRS-generation threshold energy on gas pressure.

Figure 4 shows in more detail the dependence on pressure of the threshold of the first vibrational Stokes generation. In agreement with the results shown in Fig. 3, the lowest threshold was observed in CH_4, and the threshold in H_2 was slightly lower than in D_2. If pressure p is increased, the threshold will decrease for all gases, whereas for H_2, D_2, and HD this dependence is roughly proportional to $1/p$. This dependence is due mostly to a linear decrease of the molecular coherence time, T_2, with increasing pressure.

We can follow these dependences even better if we compare the theoretical and experimental threshold values summarized in Table 1. We note that the low threshold observed in CH_4 correlates very well with the theoretical prediction. In general, our experimental values are in good agreement with the theoretically estimated values, even if the present theory does not account for any of the accompanying nonlinear effects.

When the pump energy exceeded the threshold by a factor of 2–3 we observed emission at wavelengths corresponding to higher Stokes and anti-Stokes components. In H_2 at pressures up to 4×10^6 Pa the maximum efficiency of higher Stokes components was a few percent. At the output of the Raman cell the corresponding beams were propagating in a cone centered about the direction of the pump beam. This special beam shape was caused by wave matching between the pump beam and the scattered beams.[22] However, when the pressure of H_2 was increased to 7×10^6 Pa the energy of the second Stokes component increased to as much as 12% of the pump energy, and the beam was propagating in the same direction as the pump. The third Stokes component as well as the first and the second anti-Stokes components was generated in a cone with an efficiency of 1–3%.

Table 2 summarizes several Stokes and anti-Stokes wavelengths that are due to vibrational, rotational, and vibrational–rotational components in the gases investigated. To excite rotational and vibrational-rotational components we used circularly polarized pulses.[24] The most efficient generation of rotational Stokes and anti-

Table 2. Wavelengths of Vibrational–Rotational Raman Components Observed in Four Gases with Excitation Wavelength $\lambda_p = 390$ nm[a]

	SRS components (nm)																
Gas	AS2–AS1	AS2	AS2–S1	AS1–AS1	AS1	AS1–S1	O–AS1	O–S1	S1–AS1	S1	S1–S1	S2–AS1	S2	S2–S1	S3–AS1	S3	S3–S1
H_2	289	294	300	330	336	342	381	399	453	465	478	558	577	597	727	759	797
HD					342					454			544				
D_2				344	349	354		396	384	441	450	497	508	519	585	600	615
CH_4					350					440			505			592	

[a] AS1, AS2, first and second anti-Stokes, respectively; S1, S2, S3, first, second, and third Stokes, respectively; AS2–AS1, combination of first rotational anti-Stokes with second vibrational anti-Stokes.

Stokes components was observed in H_2 (Fig. 5), whereas in D_2 we observed only the Stokes components of the rotational spectrum. In CH_4 and HD no rotational components were observed. For CH_4 the rotational lines were absent because rotational scattering is forbidden by the symmetry of the molecule. For HD the rotational scattering is allowed. However, the corresponding spectral lines were absent because the amplification factor was insufficient.[25] Note that the various frequency shifts shown in Table 2 cover a broad interval from a few to several hundred inverse centimeters.

Figure 5 shows the spectrum of Stokes components in H_2, D_2, and CH_4 excited with linearly and circularly polarized light. With the linearly polarized excitation we observed as many as three higher-order vibrational Stokes components, shifted by multiples of fundamental frequencies $\Delta\nu = 4155\ \mathrm{cm}^{-1}$ (H_2), $\Delta\nu = 2997\ \mathrm{cm}^{-1}$ (D_2), and $\Delta\nu = 2917\ \mathrm{cm}^{-1}$ (CH_4). When the polarization of the pump was changed to circular, we observed rotational Stokes and anti-Stokes satellite components shifted by $\Delta\nu = 587\ \mathrm{cm}^{-1}$ (H_2) and $\Delta\nu = 414\ \mathrm{cm}^{-1}$ (D_2) with respect to the vibrational Stokes lines. For H_2 the intensity of the rotational satellites was comparable with that of the vibrational SRS lines. Properties of additional Stokes components in H_2 are discussed in Refs. 7 and 26.

As the last measurement we obtained the temporal intensity profile of the first Stokes component in three gases. We accomplished this by using noncollinear frequency-doubling autocorrelation in a 1-mm-thick BBO crystal (type 1 phase matching). Figure 6 presents the autocorrelation functions of a SRS pulse for H_2, D_2, and CH_4. For reference, the autocorrelation of the pump pulse, measured at the input to the SRS cell, is given. The energy of the pulses was 50 μJ for H_2 and D_2 and 30 μJ for CH_4. The spectrum of the first Stokes pulse in D_2 is shown in Fig. 5(c).

We observed that the duration of the SRS pulse experienced appreciable shortening with respect to the duration of the pump pulses. This effect was most pronounced in H_2 and was less obvious in CH_4. The explanation for this phenomenon may involve the fact that in the transient regime the SRS pulse is formed on the trailing edge of the pump pulse.[27] We are preparing a detailed analysis of the femtosecond SRS pulse forms, including the effects of GVM.

We mentioned above that competing nonlinear processes such as white-light-continuum generation appear

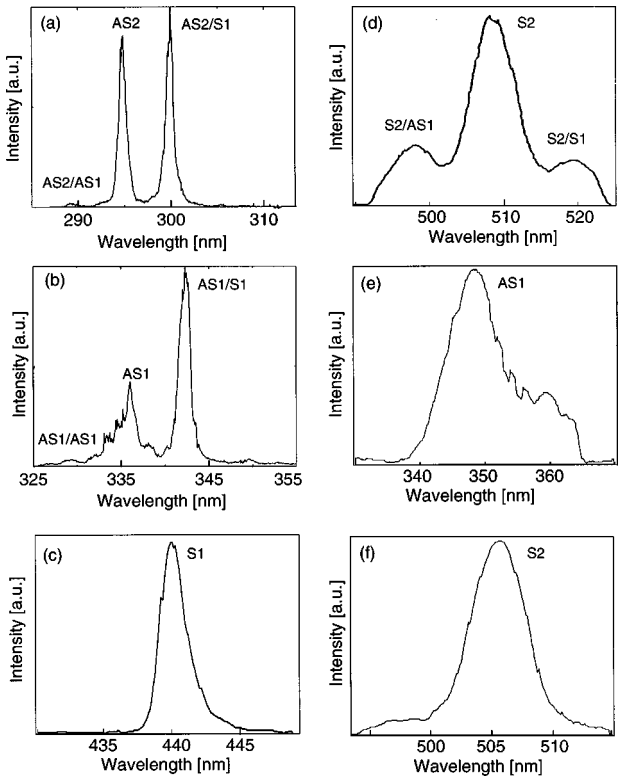

Fig. 5. Spectra of stimulated Raman components in several gases: (a) second anti-Stokes (As2) and (b) first anti-Stokes (As1) in H_2 at $p = 3 \times 10^6$ Pa; (c) first Stokes (S1) and (d) second Stokes (S2) in D_2 at $p = 4.5 \times 10^6$ Pa; (e) first anti-Stokes and (f) second Stokes in CH_4. Spectra (a), (b), and (d) are excited with a circularly polarized pump; spectra (c), (e), and (f) are excited with a linearly polarized pump.

to reduce the conversion efficiency, especially with increasing pump power. Nonlinear self-phase modulation manifests itself also as spectral broadening of the Raman lines, especially those closer to the excitation wavelength. Figure 7 illustrates this observation; for this figure we used a grating monochromator to monitor the spectral intensity profile of the radiation at the output of the cell. First we measured the spectrum of the transmitted pump (Rayleigh scattering) at several powers. Below the SRS threshold the spectrum is identical with that at the input to the cell. Above the threshold we first observe a gradual broadening of the spectral line shape to a factor of 3 to 4 (measured at half-maximum). After that the

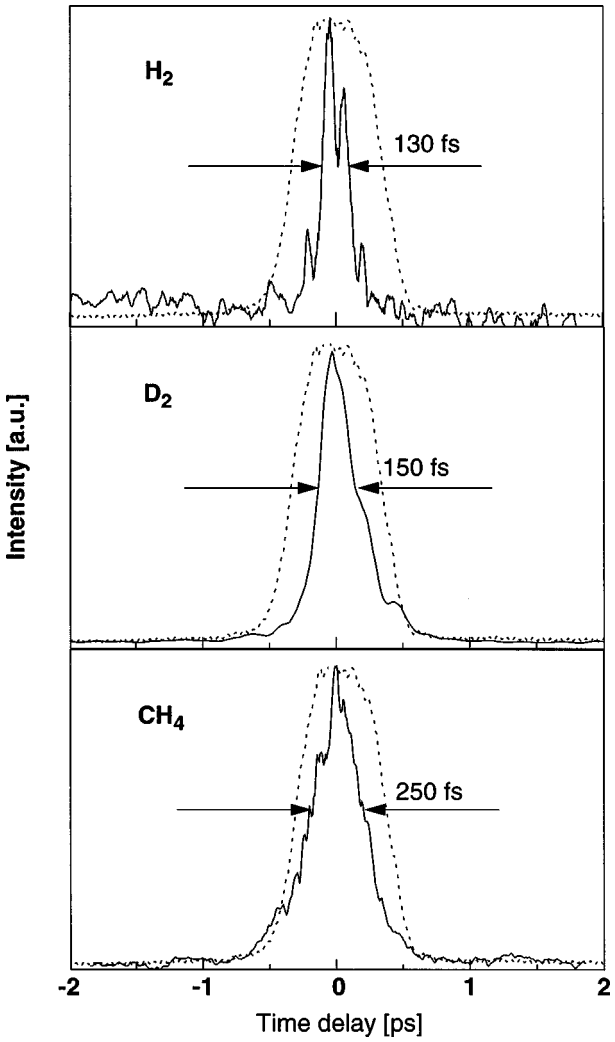

Fig. 6. Autocorrelation traces of first vibrational Stokes pulses in H_2, D_2, and CH_4 (solid curves) compared with autocorrelation of the pump pulses at the input of the SRS cell (dashed curves).

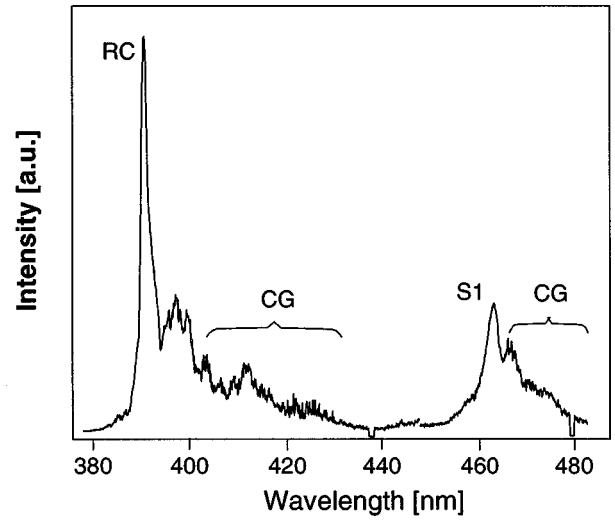

Fig. 7. Intensity spectrum of broadband SRS in H_2 at $p = 5 \times 10^6$ Pa and pump pulse energy 0.11 mJ: RC, Rayleigh scattering component; CG's, broadband spectral continua; S1, first vibrational Stokes component.

most intense part of the spectrum suddenly goes back to the initial narrow width, whereas on the Stokes side of the spectrum there appears a broad structureless background that is due to white-light generation. The average intensity and spectral extent of the broad spectral component increase with increasing the pump power, gradually filling in the gap between the pump and the first Stokes, and extend further toward higher Stokes components.

Different molecules showed different spectral behaviors as functions of pump intensity. In H_2 the Stokes lines broadened simultaneously with the broadening of the pump beam spectrum. At intensities above the white-light-generation threshold the Stokes spectrum had a similar broad wing, which was dropped off toward longer wavelengths. In CH_4, however, a much different situation was observed. In particular, the broadening of the Stokes lines started at lower pump intensities, even before the broadening in the pump beam itself occurred. In some instances we were able to observe that the width of the Stokes lines was broader than that of the pump by a factor of 3 or 4, approaching 400 cm^{-1}. Again, when the power of the pump was increased further, the Stokes lines collapsed to 100–150 cm^{-1}, and the intensity of broad background intensity dropped as well.

Considerable differences were observed also in the character of the broadening of the Rayleigh spectrum at high excitation power. In H_2 the spectrum broadened in the direction of longer wavelengths, whereas in CH_4 the broadening was mostly in the anti-Stokes region. We can attribute these peculiarities to possible different wavelength dependences of the gain factor and different values of the nonlinear index of refraction in H_2 and CH_4. The exact mechanisms of these processes will be the subject of our further investigation.

4. CONCLUSION

To summarize, we have investigated in detail the efficiency and the spectral–temporal characteristics of SRS in the femtosecond time domain for gases such as H_2, D_2, HD, and CH_4. Experimental conditions for efficient conversion of the wavelength of energetic femtosecond pulses with a possibility of choosing from among many vibrational and rotational Raman shift frequencies were determined. A 18% conversion efficiency to the first Stokes component in H_2 was achieved, despite the fact that we were dealing with a strongly transient regime. In addition, a theoretical analysis of the transient amplification factor and the SRS-generation threshold was presented for H_2, D_2, HD, and CH_4 and was in good accord with our experimental results.

Despite evidence of self-phase modulation and white-light-continuum generation at high intensities, it is possible by taking into account the properties of the various gases to apply this technique to efficient frequency conversion of commercial amplified Ti:sapphire lasers in a fairly broad spectral range, extending from the near UV to the near IR. Efficient generation of first, second, and third Stokes and anti-Stokes lines demonstrated possibility of achieving femtosecond-pulse generation in the spectral range 280–797 nm simultaneously in as many as 10

lines. The principal advantage of this technique consists in its relatively simple operation principle and high efficiency, especially when it is compared with parametric amplification in nonlinear crystals.

By analyzing the spectral characteristics of the Raman and the Rayleigh components of the signal we found evidence that self-phase modulation and white-light generation, in fact, limit the ultimate conversion efficiency. These nonlinear process, which occur at high excitation intensity, broaden the spectrum and distort the phase front of the pump pulse and thus act to deplete the intensity of the pump.

Further investigations are needed to clarify the role of competing nonlinear processes, which tend to broaden the spectrum of the SRS signal and to be responsible for limiting efficiency because of distortion of the phase front of the pump pulses.

ACKNOWLEDGMENTS

This study was supported by Russian Fund of Fundamental Investigations 97-02-18380 and by the Russian Federation State Program "Fundamental Metrology." It was carried out in the framework of the International Cooperation Program with countries of central and eastern Europe, financed by the Swiss Federal Government for Foreign Affairs through the Swiss National Science Foundation (grant 7SUPJ048609).

V. Krylov's e-mail address is Krylov @phys.chem.ethz.ch; that of A. Rebane is rebane@physics.montana.edu; and that of V. G. Bespalov is bespalov@admiral.ru.

REFERENCES

1. V. G. Bespalov, V. N. Krylov, V. N. Mikhailov, V. A. Parfenov, and D. I. Staselko, "Generating tunable radiation with high spectral luminance based on vibrational and rotational stimulated Raman scattering in gases," Opt. Spectrosc. **70**, 193–196 (1991).
2. J. G. Wessel, K. S. Repasky, and J. L. Carlsten, "Efficient seeding of a Raman amplifier with a visible laser diode," Opt. Lett. **19**, 1430–1432 (1994).
3. V. G. Bespalov, V. N. Krylov, D. I. Staselko, V. N. Sizov, V. A. Parfenov, and E. Yu. Yutanova, "Coherence and space-time structure of the Stokes radiation of stimulated Raman scattering during superregenerative amplification," Opt. Spectrosc. **63**, 742–747 (1987).
4. P. G. May and W. Sibbett, "Transient stimulated Raman scattering of femtosecond laser pulses," Appl. Phys. Lett. **43**, 624–626 (1983).
5. C. Jordan, K. Stankov, and G. Marowsky, "Compression of femtosecond light pulses by stimulated Raman scattering," in *International Quantum Electronics Conference*, Vol. 9 of 1994 OSA Technical Digest Series (Optical Society of America, Washington, D.C., 1994), p. 97.
6. J. Wang, Y. Siegel, C. Lii, E. Mazur, and J. Reintjes, "Subpicosecond stimulated Raman scattering in high-pressure hydrogen," J. Opt. Soc. Am. B **11**, 1031–1037 (1994).
7. V. Krylov, A. Rebane, D. Erni, O. Ollikainen, U. Wild, V. Bespalov, and D. Staselko, "Stimulated Raman scattering in hydrogen by frequency-doubled amplified femtosecond Ti:sapphire laser pulses," Opt. Lett. **21**, 381–383 (1996).
8. R. L. Carman, F. Shimizu, C. S. Wang, and N. Bloembergen, "Theory of Stokes pulse shapes in transient stimulated Raman scattering," Phys. Rev. A **2**, 60–72 (1970).
9. N. J. Everall, J. P. Partanen, J. R. M. Barr, and M. J. Shaw, "Threshold measurements of stimulated Raman scattering in gases using picosecond KrF laser pulses," Opt. Commun. **64**, 393–397 (1987).
10. A. Yariv, *Quantum Electronics*, 2nd ed. (Wiley, New York, 1975).
11. A. Penzkofer, A. Laubereau, and W. Kaiser, "High intensity Raman interactions," Prog. Quantum Electron. **6**, 55–140 (1979).
12. M. D. Duncan, R. Mahon, L. L. Tankersley, and J. Reintjes, "Transient stimulated Raman amplification in hydrogen," J. Opt. Soc. Am. B **5**, 37–52 (1988).
13. W. K. Bishel and M. J. Dyer, "Wavelength dependence of the absolute Raman gain coefficient for the $Q(1)$ transition in H_2," J. Opt. Soc. Am. B **3**, 677–682 (1986).
14. W. K. Bishel and G. Black, "Wavelength dependence of the Raman scattering cross section from 200–600 nm," in *Excimer Lasers—1983*, C. K. Rhodes, H. Egger, and H. Pummer eds. (American Institute of Physics, New York, 1983), pp. 181–187.
15. J. R. Murray and A. Javan, "Effect of collision on Raman line profiles of hydrogen and deuterium gas," J. Mol. Spectrosc. **42**, 1–26 (1972).
16. G. J. Rosasco, A. D. May, W. S. Hurst, L. B. Petway, and K. C. Smyth, "Broadening and shifting of the Raman Q branch of HD," J. Chem. Phys. **90**, 2115–2124 (1989).
17. Y. Taira, K. Ide, and H. Takuma, "Accurate measurement of the pressure broadening of the $v1$ Raman line of CH_4 in the 1–50 bar region by inverse Raman spectroscopy," Chem. Phys. Lett. **91**, 299–301 (1982).
18. J. J. Ottusch and D. A. Rockwell, "Measurement of Raman gain coefficients of hydrogen, deuterium, and methane," IEEE J. Quantum Electron. **24**, 2076–2080 (1988).
19. D. A. Haner and I. S. McDermid, "Stimulated Raman shifting of the Nd:YAG fourth harmonic (266 nm) in H_2, HD and D_2," IEEE J. Quantum Electron. **26**, 1292–1298 (1990).
20. M. Born and E. Wolf, *Principles of Optics* (Pergamon, Oxford, 1993).
21. T. Larsen, "Dispersion," in *Optische Konstanten*, Vol. 8 of Landolt–Bornsten Zahlenwerte und Funktionen, K.-H. Helwege and A. M. Helwege, eds. (Springer-Verlag, Berlin, 1962), pp. 885–887.
22. V. S. Butylkin, A. E. Kaplan, Yu. G. Khronopulo, and E. I. Yakubovich, *Resonant Nonlinear Interactions of Light with Matter* (Springer-Verlag, Berlin, 1989).
23. V. Krylov, A. Rebane, A. G. Kalintsev, H. Schwoerer, and U. P. Wild, "Second-harmonic generation of amplified femtosecond Ti:sapphire laser pulses," Opt. Lett. **20**, 198–200 (1995).
24. H. Kawano, Y. Hirakawa, and T. Imasaka, "Generation of more than 40 rotational Raman lines by picosecond and femtosecond Ti:sapphire laser for Fourier synthesis," Appl. Phys. B: Lasers Opt. **65**, 1–4 (1997).
25. F. Hanson and P. Poirier, "Stimulated rotational Raman conversion in H_2, D_2 and HD," IEEE J. Quantum Electron. **29**, 2342–2345 (1993).
26. V. Krylov, A. Rebane, D. Erni, O. Ollikainen, U. Wild, V. Bespalov, and D. Staselko, "Stimulated Raman amplification of femtosecond pulses in hydrogen gas," Opt. Lett. **21**, 2005–2007 (1996).
27. W. H. Lowdermilk and G. I. Kachen, "Coherent transient pulse propagation," Opt. Commun. **18**, 68–69 (1976).